International Journal of Mass Spectrometry 285 (2009) 1–11

Contents lists available at ScienceDirect

International Journal of Mass Spectrometry

journal homepage: www.elsevier.com/locate/ijms

Development of a novel technique for quantitatively determining the products of electron-ion dissociative recombination

Christopher D. Molek, Viktoriya Poterya, Nigel G. Adams*, Jason L. McLain

Department of Chemistry, University of Georgia, Athens, GA 30602, USA

ARTICLE INFO

Article history:
Received 20 December 2008
Received in revised form 17 February 2009
Accepted 17 February 2009
Available online 1 April 2009

Keywords:
Dissociative recombination
CH5+
Product of recombination
Electron-ion recombination
Ion–ion recombination

ABSTRACT

Dissociative electron-ion recombination (DR) is an important ionization loss process and source of neutral reactive radicals in the interstellar medium (ISM) and many other molecular plasmas. Unfortunately, neutral products are difficult to identify with only about 40 distributions being reported in the literature. These have been obtained by spectroscopic techniques integrated with flowing afterglows (FA) and using storage rings (SR). The data obtained by SR measurements are more extensive than those determined in the FA. Some data are available where the two techniques overlap, however here there are very significant differences. To resolve these contradictions, a new technique to quantitatively detect product neutrals has been developed.

This technique is based on the FA and uses an electron impact (EI) ionizer to ionize the neutral products prior to detection by a quadrupole mass filter/electron multiplier. Two experimental methodologies, both using pulsed gas techniques, isolate and quantify the DR products. In one approach, an electron attaching gas is pulsed into the flow to transiently destroy electrons and thus quench DR. N_2H^+ recombination has been used as a test case and results from this approach give an upper limit of 5% for the NH + N product channel, the remainder being N_2 + H. In the second approach, the reagent gas N_2 is pulsed. Here the absolute percentages of products are monitored versus initial N_2 concentration. Results from this approach also give an upper limit of 5% for NH + N production. This establishes that N_2 + H is the dominant channel, being at least 95%, and that there is no significant NH production. This was contrary to a recent storage ring measurement which yielded 64% NH + N and 36% N_2 + H. Note, that these values have changed due to a recent re-measurement of the DR revealing that the NH channel is not nearly as significant as originally thought. Additionally, the DR product distribution for CH_5^+ is reported and discussed.

1. Introduction

Dissociative electron-ion recombination (DR) is very important, since it is a dominant loss process in many molecular plasma media, such as interstellar gas clouds [1], cometary coma [2,3], planetary atmospheres [2,4], combustion flames [5], etc. One important reason is that DR is generally much more rapid than other recombination processes (radiative, dielectronic, collisional radiative) [6]. Because of this, and to try to understand the DR process, there has been a body of experimental data gathered (temperature dependencies of the rate coefficients, quantitative determination of the products, and determination of states of excitation in the products). These data have contributed to the understanding of the reaction mechanisms involved. The mechanisms will not be discussed in detail here and the reader is referred to recent reviews [7–10].

In spite of the limited data (partly due to the experimental challenge), there has been a considerable effort to determining the products of DR. Currently, there are two main techniques used to determine the product distributions; these are the flowing afterglow (FA) and the storage ring (SR). Initially, the FA was used to identify products via vuv absorption spectroscopy and laser induced fluorescence (LIF) [11–13], where these techniques were used to obtained the H-atom contribution to the full product distribution in the recombinations of N_2H^+, HCO^+, HCO_2^+, N_2OH^+, $OCSH^+$, H_2CN^+, H_3O^+, H_3S^+, NH_4^+, and CH_5^+ [13]. Additionally, the H-atom, O-atom, and OH products of HCO_2^+, N_2OH^+, and H_3O^+ recombination were determined directly and indirectly using laser induced fluorescence [12,14,15]. Although the FA has the strength of chemical versatility, there are difficulties associated with this experimental technique when using spectroscopic detection. In particular, the need for multiple quantitative spectroscopic techniques for the different products makes a full distribution difficult to obtain and very time consuming.

However, the storage ring has its own set of difficulties. To obtain product distributions and rate constants using this technique, a

* Corresponding author. Tel.: +1 706 542 3722; fax: +1 706 542 9454.
E-mail address: adams@chem.uga.edu (N.G. Adams).

1387-3806/$ – see front matter © 2009 Elsevier B.V. All rights reserved.
doi:10.1016/j.ijms.2009.02.031

Table 1
Listing of previous flowing afterglow spectroscopic measurements and storage ring measurements of the product distributions for H_2O^+ (FA [27,68] and SR [69–71]), H_3O^+ (FA [15] and SR [69,72–74]), and N_2H^+ (FA [13] and SR [24]). Note that a remeasurement by SR shows the NH channel in the N_2H^+ DR to be lower than previously found [9].

	FA		SR		
$H_2O^+ + e^- \rightarrow H + OH + 714$ kJ/mol (7.4 eV)	55%	55%	22%	30%	20%
$H_2O^+ + e^- \rightarrow O + H_2 + 733$ kJ/mol (7.4 eV)	<23%	<21%	10%	13%	9%
$H_2O^+ + e^- \rightarrow O + 2H + 299$ kJ/mol (3.1 eV)	>22%	>24%	68%	57%	71%
$H_3O^+ + e^- \rightarrow H_2O + H + 617$ kJ/mol (6.4 eV)	5%		33%	18%	25%
$H_3O^+ + e^- \rightarrow OH + H_2 + 550$ kJ/mol (5.7 eV)	36%		18%	11%	14%
$H_3O^+ + e^- \rightarrow OH + 2H + 125$ kJ/mol (1.3 eV)	29%		48%	67%	60%
$H_3O^+ + e^- \rightarrow O + H + H_2 + 135$ kJ/mol (1.4 eV)	30%		1%	4%	1.3%
$N_2H^+ + e^- \rightarrow N_2 + H + 817$ kJ/mol (8.5 eV)	~100%		36%		
$N_2H^+ + e^- \rightarrow NH + N + 217$ kJ/mol (2.3 eV)	~0%		64%		

detailed and involved analysis needs to be employed, including corrections for collisions with background gases [16–18], iterative correction for the regions of merging and de-merging of the ion and electron beams [19], and allowance for anisotropic angular distribution of reaction products [20]. Also, in the SR, the ability to distinguish between products 1 amu apart in mass diminishes for heavier products (e.g., C_nH_m, where $n \geq 2$). This is unfortunate since heavier hydrocarbon chemistry is extremely important, for both the ions and neutrals in the Titan atmosphere and in the ISM [21,22]. For example for $C_2H_4^+$, the counts versus energy for the various neutral fragments were not fully resolved in the SR and the overlapping peaks needed to be fitted using Gaussian profiles [23]. The full resolution for this number of carbons was still not obtained even using deuterated ions, e.g., $C_2D_5^+$ [24]. For $C_3H_4^+$, $C_4H_5^+$ and $C_4H_9^+$, SR experiments have not resolved the H-atom contribution to the products at all (with only DR products with 1, 2, or 3 carbon atoms being distinguished) [25,26]. Also, in most cases, specific recombination product distributions have only been determined by a single SR or FA group. However in a few instances, where measurements have been made by the FA and SR, namely for H_2O^+, H_3O^+, and N_2H^+, there are discrepancies. These product distributions are given in Table 1, where substantial differences are seen between the two techniques.

For H_2O^+ DR, see Table 1, the differences between the distributions have been attributed to vibrational excitation of the recombining ions in the FA, which could not be relaxed by resonant charge transfer. This was because it has to compete with the reaction which forms H_3O^+, see Eqs. (1) and (2) [27].

$$H_2O^{+*} + H_2O \rightarrow H_2O^* + H_2O^+ \quad (1)$$

$$H_2O^{+*} + H_2O \rightarrow H_3O^+ + OH \quad (2)$$

Note that the variation between different SR measurements is smaller but certainly not negligible. In the FA for H_3O^+ DR, it was ensured that the recombining ions were vibrationally relaxed using resonant proton transfer where there are no competing channels, i.e.,

$$H_3O^{+*} + H_2O \rightarrow H_2O^* + H_3O^+ \quad (3)$$

But even with the H_3O^+ vibrationally relaxed, there are still marked differences between the various measured distributions using the two techniques, see Table 1. The situation was equally bad for N_2H^+ recombination. Note that a remeasurement by SR shows the NH channel in the N_2H^+ DR to be lower than previously found. Thus, there is an obvious need for a new and independent technique and this is the subject of the present paper. The technique devised uses the FA, because of its chemical versatility, in conjunction with electron impact ionization and mass spectrometric analysis to detect the DR products with selectivity and sensitivity (achieved using pulsed counting). Thus, unlike the spectroscopic measurements used previously, this enables multiple product channels to be monitored with a single measurement technique. Also, with mass spectrometry 1 amu or better resolution can readily be achieved, giving the ability to study the individual products from DR of larger hydrocarbons. An additional strength of this approach is that it is sensitive to small signals in the presence of a large background. However, note that at the electron energy typically used for ionization (70 eV), there is some fragmentation of the sample that is being ionized, but since there is a wealth of data on the degree of fragmentation at this energy, this can be accounted for. The distinction between the ionization products of DR (signal) and residual background gases is achieved by pulsed addition of electron attaching or other gases.

2. Experimental

The generic FA technique has been described in detail previously [28,29] and will only be briefly discussed here; where features are different they will be emphasized, see Fig. 1. This new technique involves two experimental approaches, which both utilize a FA plasma and these are described using N_2H^+ DR as an example. A separate experiment to determine the products of DR for CH_5^+ utilizes only one approach.

The recombining ions are generated using a typical flow tube pressure of 1.4–1.5 Torr with a He flow rate of 16.0 slm; at this pressure the diffusive losses are not very significant and most of the He^+ has been converted to He_2^+ by the ternary reaction, Eq. (4), before the other gases are added to the flow tube. Note that

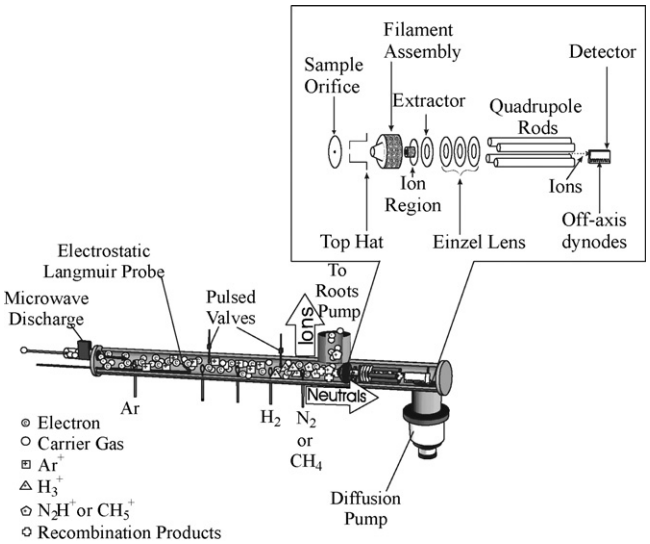

Fig. 1. Schematic of the flowing afterglow (FA) with expanded view of the ionization and ion focusing section of the detection system. The sample orifice is a 5×10^{-2} mm diameter hole that allows passage of either ions or neutrals, depending on the mode of operation. Also shown are the different positions of gas addition (Ar, H_2, and N_2 or CH_4) and the pulsed valve positions.

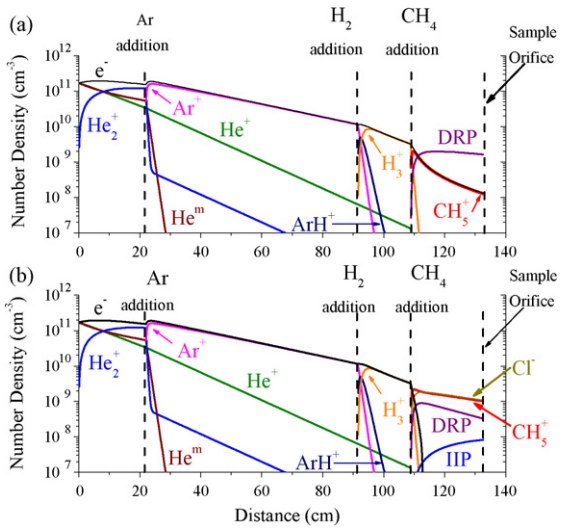

Fig. 2. Kinetic model of the CH_5^+ plasma as a function of distance down the flow tube from 0 cm, the microwave discharge source. (a) Is without CCl_4 and (b) is with CCl_4. The total dissociative recombination products (DRP) and ion–ion products (IIP) are included in the model. There are three gas additions points for argon, hydrogen, and methane to generate the recombining ion under study, CH_5^+. Also shown as a dotted line is the sampling orifice, where the neutrals are separated from the ions.

both 16.0 slm and 31.4 slm were used for the N_2H^+ DR study (see Section 3.2). The He is 99.997% pure and is further purified with two liquid N_2 cooled sieve traps. Argon gas (99.999%) is added to the flow tube ~22 cm downstream of the microwave discharge through a ring port at a concentration of $\sim 1.6 \times 10^{14}$ molecules/cm^3, which destroys He^m and He_2^+ (generating Ar^+) and has the bonus of increasing the ionization number density. Further downstream (~70 cm) from the Ar addition, H_2 (99.999% purity, further purified by a liquid N_2 cooled sieve trap) is added at a concentration of $\sim 1 \times 10^{13}$ molecules/cm^3 to quickly create an H_3^+/e^- plasma. Approximately 17 cm downstream of the H_2 addition, the reagent gas of interest is added, in these cases N_2 (99.999% purity) or CH_4 (99.97% purity), at concentrations of $\sim 5 \times 10^{12}$ molecules/cm^3. This forms the recombining ion of interest, either N_2H^+ or CH_5^+ by proton transfer. Eqs. (4)–(7) summarize the chemical reactions leading up to H_3^+, which readily proton transfers to N_2 and CH_4, with respective rates of 1.6×10^{-9} cm^3 s^{-1} and 2.4×10^{-9} cm^3 s^{-1} [30].

$$He^+ + He + He \rightarrow He_2^+ + He \quad k = 2.0 \times 10^{-31}\ \text{cm}^6\ \text{s}^{-1} \tag{4}$$

$$He_2^+ + Ar \rightarrow Ar^+ + 2He \quad k = 2.0 \times 10^{-10}\ \text{cm}^3\ \text{s}^{-1} \tag{5}$$

$$Ar^+ + H_2 \rightarrow ArH^+ + H \quad k = 8.6 \times 10^{-10}\ \text{cm}^3\ \text{s}^{-1} \tag{6}$$

$$ArH^+ + H_2 \rightarrow H_3^+ + H \quad k = 6.3 \times 10^{-10}\ \text{cm}^3\ \text{s}^{-1} \tag{7}$$

Kinetic data in Eqs. (4)–(7) are from literature [30,31]. A kinetic model showing the variations of the ion signals with distance along the flow tube for the production and recombination of CH_5^+ (for both the absence and presence of CCl_4) is shown in Fig. 2. The formations of N_2H^+ and CH_5^+ are monitored using the quadrupole mass spectrometer to ensure that the ion under study is the dominant plasma ion. Two experimental approaches are used to determine the product distributions. Both use a pulsed gas technique to modulate DR by pulsing (i) the reagent gas (N_2 or CH_4) or (ii) an electron attaching gas, which quenches DR. Both pulsed gas techniques are similar to those previously used for detecting spectroscopic emissions from DR [32,33]. In this way, DR products are distinguished from other neutrals such as unreacted reagent gases which are unaffected by the modulation. Note that, the DR product neutrals, which are detected, have been thermalized kinetically by collisions with the He buffer gas. Vibrational and rotational deexcitation can also occur by such collisions or by radiative relaxation. Clean pulsing of the modulated gas is critical for determining DR products and is achieved by adjusting He flushes upstream and downstream of a pulsing valve. A detailed description and a schematic of this arrangement can be found in Mostefaoui et al. and Williams et al. [32,33]. The detection of the DR products in this way required some modifications to the existing FA system.

2.1. Modifications to the flowing afterglow

The quantitative identification of DR products is carried out using the pulsed gas techniques mentioned above. In order to detect the products an axial electron impact ionizer (Extrel Axial Molecular Beam Ionizer with thoriated iridium filaments) was positioned in front of a downstream quadrupole mass filter to ionize the sampled neutrals (products of DR and background gases); these are termed monitor ions. Note that, in order to monitor the plasma ions as described earlier, the potentials on the sample orifice and top hat lens are near ground or biased negative to allow passage of these positive ions into the detection system. In addition, the electron impact ionizer is off and appropriate voltages are applied to an Einzel lens to focus the plasma ions into the quadrupole. To prevent plasma ions and electrons from entering the detection system, small bias voltages are applied to the sample orifice (~+0.5 V) and top hat lens (~−0.5 V) just upstream of the axial ionizer. Neutrals can still pass into the detection system and the DR products, and other neutrals being sampled, are distinguished by pulse modulation (~1 Hz) of either an electron attaching gas or the reactant gas into the flow tube, discussed in detail in the next two sections. After ionization, the monitor ions are focused and injected into the quadrupole by a series of lenses, see Fig. 1. Ions passing through the quadrupole filter are detected by a discrete dynode electron multiplier (ETP model AF553H). To prevent interference from radiation coming from the flow tube, specifically from the upstream microwave source, the dynodes of the multiplier are off-axis from the quadrupole exit. The microwave discharge producing the plasma is also off axis from the flow tube. After the multiplier, the ion pulses are amplified by an Ortec fast timing preamplifier (VT120C with a gain of 20 and a 10–350 MHz bandwidth), pulse height discriminated, and counted in a Stanford Research Systems (SR400) gated counter (GC). Since the background counts are often much larger than the signal counts, the current output response of the multiplier must increase linearly as the count rate increases up to high count rates. The ETP model has a large dynamic range where the deviation from linearity is near zero for up to 70 μamps of output current. This output current (I) when converted to counts per second establishes the count rate saturation limit for the detector, i.e., for a typical gain of $\sim 1 \times 10^7$, which occurs at a voltage of ~1.8 kV applied across the 21 stage dynode stack, the maximum count rate is $\sim 5 \times 10^7$ counts/s. In the experiments, count rates are kept below this value to avoid errors due to multiplier saturation. The data collection cycles at twice (~2 Hz) the frequency of the pulsed gas modulation (~1 Hz) with data being collected when the pulsed gas is out (A) and when the pulsed gas is in (B). A timing circuit was devised to manage the data collection so that A can be separated from B when both are passed through a single circuit in the GC (see Fig. 3). This was necessary since, using the dual channel mode in the GC sends the A and B counts through different circuitry (independent gates and discriminators), thus causing erroneous results due to the slight mismatch of the channel circuitry used to collect the counts for A and for B. Therefore, this mode cannot be used and a single channel to collect both A and B was necessary. The separation of A and B is made using the odd (B) and even (A) memory bins of the 2000 bin memory in the GC. The circuit coordinates the data collection so that the A data and B data are put in the appropriate separate memory bins. When the circuit is armed, the GC trigger is at TTL low until the first ris-

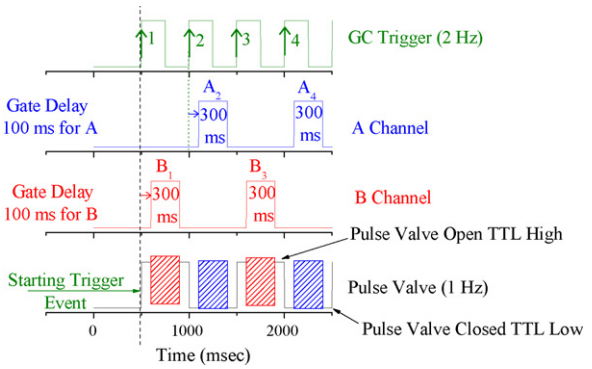

Fig. 3. Pulse valve timing diagram used for the accumulation of data in channels A and B. Note, GC refers to a gated counter (SR400). The red rectangles on the pulse valve TTL (for triggers 1, 3, etc.) represent the counting for the odd memory bins (B_1, B_3,. . .B_{1999}) of the GC and the blue rectangles on the pulse valve TTL (for triggers 2, 4, etc.) are counting for the even memory bins (A_2, A_4,. . .A_{2000}). Vertical green arrows indicate GC triggers. (For interpretation of the references to color in this figure legend, the reader is referred to the web version of the article.)

Table 2
Absolute fractions for the electron impact fragmentation patterns (70 eV) of N_2 and NH that were used in the N_2H^+ studies. Fragmentation for N_2 is calculated from fragmentation patterns [34] and NH from the ratio of relative ionization cross sections (fragment to parent) [75].

N_2		NH	
Ion	Absolute fraction	Ion	Absolute fraction
N_2^+	0.85	NH^+	0.78
N^+	0.15	N^+	0.22

ing edge of the pulse valve cycle, from which a GC trigger signal starts (this operates at twice the frequency of the pulse valve). In this way, the odd memory bins are always correlated to when the pulsed gas is in the flow tube (B_1, B_3,. . .B_{1999}) and the even memory bins correspond to when the pulsed gas is out (A_2, A_4,. . .A_{2000}), see Fig. 3. Additionally, a delay is used before counting so that data is not being collected near the pulse valve transitions. Counting is also stopped early in order to avoid the transition as well. These non-counting periods are ~10% of the pulse valve period.

Electron impact ionization (Extrel Axial Ionizer) of the neutrals is made using an electron energy of 70 eV, which takes advantage of the wealth of experimental data available in the literature for this electron energy, but mainly of stable species [34]. For radical species, relative fragmentation patterns are obtained from the ratio of the fragment ion to parent ion ionization cross sections, which are readily available [35]. From the relative fragmentation patterns, the absolute percentages are calculated and given in Tables 2 and 3. Data for N_2 and NH are given in Table 2 and those for CH_4, CH_3, CH_2, and CH are given in Table 3. Note that the two question marks in Table 3 indicate values that are not known. These values are expected to be small for two reasons. First the fragmentation of CH_4 to C^+ is only 0.02 and it is not unreasonable to assume that the C^+ fragments from CH_3 and CH_2 will also be small. Secondly, the experimental measurement of the ionization cross section for C^+ channel from CH_2 was not made because it was too small [36].

2.2. Electron-attaching gas method

For the electron-attaching gas method, a rapidly electron attaching gas (CCl_4) is pulsed into the flow tube ~10 cm upstream of the reagent gas port so that 80–90% of the electrons are attached at the point of introducing the reagent gas. Thus with attaching gas added, the DR is almost completely quenched at the addition point of N_2 or CH_4.

$$CCl_4 + e^- \rightarrow Cl^- + CCl_3 \quad (8a)$$

$$CCl_3 + e^- \rightarrow Cl^- + CCl_2 \quad (8b)$$

Then, the differences between the two pulsed situations are the signals from products of the DR. Also any impurity in the flow tube has a constant value and is cancelled out when accumulating signal, because of the difference between the pulsed gas out (A_{n+1}) versus in (B_n) is used so that,

$$S_{n+1,n} = A_{n+1} - B_n; \quad n = 1, 3, 5, \ldots \quad (9)$$

A statistically significant S is obtained by integrating S from multiple pulsed periods,

$$S = \sum_{n=1,3,5,\ldots}^{N} S_{n+1,n} = \sum_{n=1,3,5,\ldots}^{N} (A_{n+1} - B_n) \quad (10)$$

Since the counts in (A_{n+1}) are determined after the counts in (B_n), the system needs to be as stable as possible between these two periods. The concentration of attaching gas is critical; enough needs to be added to maximize signal contribution from DR between the two channels (A and B), while keeping any ion–ion recombination (iir) between the anion (Cl^-) and recombining ion of interest at a minimum. This situation is achieved by monitoring the current profile (proportional to electron density) to the movable Langmuir probe, which is at a constant DC voltage (~+3 V with respect to the flow tube). During this measurement, the probe is at a fixed position in the flow tube (i.e., the addition point of N_2 or CH_4). The amount of attaching gas added is sufficiently small so that it does not influence the ion chemistry or change the diffusive loss since it is ensured that there is still enough electron density remaining for ambipolar diffusion to be dominated by the electrons [37]. Note that any products of iir will result in a negative S and, if they occur at the same mass as a DR product, they will erroneously reduce the DR contributions at this mass. The rate constants of these particular iir are not known and therefore cannot be modeled. However, Cl will be contained in the products (Cl, HCl, NCl, CH_3Cl, CH_2Cl, etc.) and this is probed. In fact, it is shown later that Cl containing products are very minor (<2% of total products detected), thus showing that

Table 3
Absolute fractions for the electron impact fragmentation patterns (70 eV) of CH_4, CH_3, CH_2, and CH that were used for the CH_5^+ study. CH_4 is calculated from reference [34] and CH_2 and CH from the ratios of relative ionization cross sections (fragment to parent) [36]. CH_3 is calculated from measurements made in our laboratory. The question marks indicate values that are not available but are expected to be small considering that C^+ is only 0.02 from CH_4, see text. Even so, this is taken into account in the error analysis, see Section 3.6.

Ion	CH_4 Absolute fraction	CH_3 Absolute fraction	CH_2 Absolute fraction	CH Absolute fraction
CH_4^+	0.44			
CH_3^+	0.40	0.75		
CH_2^+	0.09	0.18	0.71	
CH^+	0.05	0.07	0.29	0.79
C^+	0.02	?	?	0.21

iir is slow. Even so, this small effect is accounted for in the analysis. Results from previous work and the present work demonstrate clean pulsing even with sticky gases like H_2O. See also the electron current profile, for pulsing CCl_4 in Section 3 for further details.

2.3. Pulsed reagent gas (RG) method

In the pulsed reagent gas (RG) method, the main differences from the electron-attaching gas method are the gas being pulsed and the flow tube pressure. Also, the addition points of gases are changed to ensure that the recombining ion of interest is formed further upstream to maximize signal coming from the products. Here, the reagent gas is pulsed instead of the electron attaching gas. The flow tube operates at 3.0–4.0 Torr with a He flow rate of 31.4 slm. Ar and H_2 gases are added ~22 cm downstream of the microwave discharge at concentrations of $\sim 2 \times 10^{14}$ and 5×10^{11} molecules/cm^3, respectively. The amount of H_2 added is such that the H_3^+ recombination rate coefficient is kept small ($\sim 4 \times 10^{-8}$ cm^3 s^{-1}) [38]. Approximately 24 cm downstream from the H_2 addition point, the reagent gas of interest is pulsed into the flow tube, e.g., N_2 for N_2H^+ DR. [N_2] is varied over a wide range from $\sim 8 \times 10^9$ molecules/cm^3 to $\sim 1 \times 10^{14}$ molecules/cm^3. This concentration range is such that the electron density [e] at the pulse addition point ($\sim 3.0 \times 10^{10}$ molecules/cm^3) is within this range, see Section 3 for details. To achieve the lowest concentrations of N_2, a 0.2% N_2 in He mix was used. For the higher concentrations, pure N_2 is used. Again, Eqs. (4)–(7) summarize the chemical reactions leading up to H_3^+, which then readily proton transfers to N_2 forming the recombining ion of interest, N_2H^+. Inherent in this method is that at large N_2 concentrations ([N_2] > [e]) not all of the pulsed gas will be protonated, and thus the background interferes with the detection of some of the DR neutral products. Since this interference cannot be removed by difference (unlike the attaching gas method), the flow tube conditions are chosen so that the contribution of DR products to the overall signal is varied. Here, the overall signal for N_2 is the combination of DR products and the contribution of the unreacted reagent gas. For NH and N, the overall signals are a sum of DR products and fragmentation contributions from larger mass neutrals (both unreacted reagent gas and DR product). The extraction of the percent DR product contributions from the overall signal requires modeling of the chemistry. The contributions of DR products to the overall detected monitor ions are distinguished by modeling the absolute fraction of each monitor ion as a function of initial N_2 concentration. The product distribution percentages in the model are adjusted to give a best fit to the experimental data obtained over the same range of initial N_2 concentration. This method is more complicated, yet the advantage is that ion–ion recombination is eliminated since anions cannot form.

3. Results and discussion

3.1. Experimental checks

In this section, ways of minimizing systematic error and increasing the sensitivity of the technique (i.e., signal to background sensitivity) are discussed. There are two important conditions that minimize error. Firstly, the pulsing needs to be clean and consistent. Secondly, there should be no evidence for signal build up when there is no difference between the *A* and *B* situations (i.e., where there is intentionally no difference between the pulse valve open and closed). Such a difference can occur if, for example, there is any significant drift in the gas flows.

Clean pulsing of very sticky gases can be achieved by varying the amount of He in the upstream and downstream flushes of the pulsed gas system [33]. It can be optimized by monitoring the profile of the Langmuir probe current [e$^-$] variation, as a function of time for pulsing in a 1% mix of CCl_4 in He as is illustrated in Fig. 4. The optimum profile is a clean reproducible transition (i.e., ~square wave) between the two pulse valve states (open versus closed).

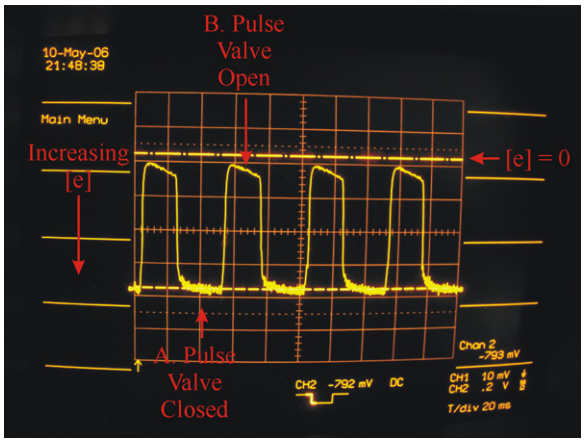

Fig. 4. Oscilloscope trace of the variation, with time, of the electron current measured with a Langmuir probe in the plasma. The current is measured by placing a small voltage (+3.0 V) on the probe, with it positioned where the reagent gas of interest is added to the flow tube. The difference observed is created by pulsing in a rapidly electron attaching gas (e.g., CCl_4). This ensures that clean, square modulation of the electron density occurs where the recombining ion of interest is forming. In this way, DR is sequentially allowed and quenched.

The second way to minimize error is to ensure that there is no signal build up when there is no difference between the two pulse valve states. This is achieved by following monitor ion masses of the products of the DR of interest while the plasma is off, i.e., with no DR occurring. By doing this, it is ensured that there are no impurities in the pulsed electron attaching gas mix that would cause interference with the monitor ion (e.g., O^+ from H_2O overlapping with CH_4^+ from CH_4). This type of error is avoided by using extremely pure gases (in the ppm range) in the mixes of the pulsed gas. This small impurity concentration in the flow tube cannot compete with the reagent gas for a proton in the proton transfer reaction and thus will not interfere with the formation of the ion under study. For these conditions, data of the kind illustrated in Fig. 5 is obtained, which is a test for signal build up when the plasma is off. These data were collected under the same conditions as used for the CH_5^+ DR study (i.e., Ar,

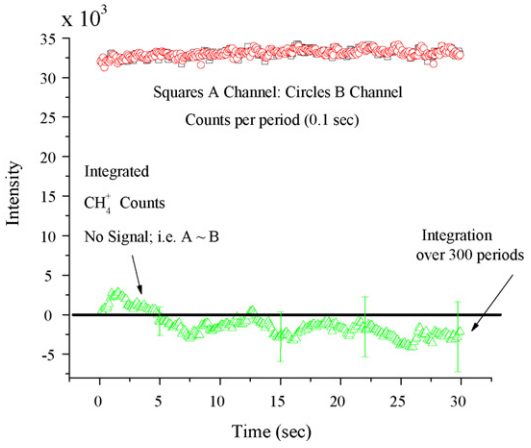

Fig. 5. A test to detect any erroneous signal build-up when no signal is present. The conditions under which these data were collected are the same gas flow conditions as in the CH_5^+ DR study, but with no plasma ionization. The CH_4^+ monitor ion signal is created by electron impact ionization of CH_4. It can be seen that the integrated signal ($\sum$(A–B)) just oscillates close to the zero due to the random errors associated with counting and does not build up.

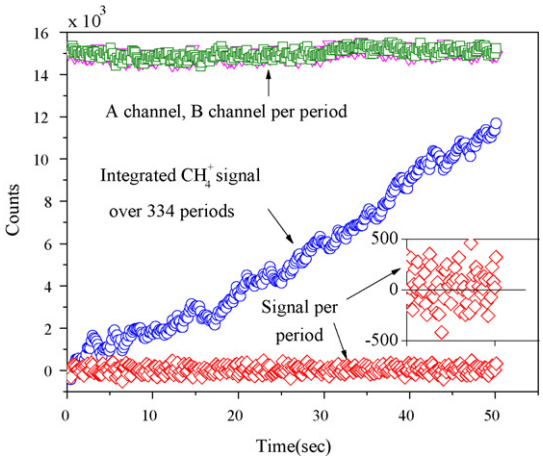

Fig. 6. A sensitivity test to detect a small amount of CH_4 pulsed into the flow tube where there is a large constant background of CH_4 (i.e., S/BG $\sim 10^{-3}$). This is done by monitoring the CH_4 using electron impact ionization to create a CH_4^+ monitor ion. Channels A (green squares) and B (purple inverted triangles) are individual periods where the pulsed gas is in and out. There is very little difference between these counts denoted by signal (S = A–B, red diamonds) and the magnified inset of the figure shows how close the signal per period is to the zero. However the integrated signal (blue circles) is clearly seen to build up by exactly the amount expected. Note that the integrated signal is inverted so that it builds in the positive direction for illustrative purposes (For interpretation of the references to color in this figure legend, the reader is referred to the web version of the article).

H_2, CCl_4 and CH_4 added to the flow), but with the plasma off. The red circles (Channel A, pulse valve closed) and black squares (Channel B, pulse valve open; squares are under the circles) are plotted as counts per period, 0.1 s, versus time in seconds. The green triangles (CH_4^+ counts) represent the integration up to 300 periods of the CH_4^+ signal. It should be noted that the A and B channels are very stable. The counts from CH_4^+ do not have any significant build up and variations in the integrated signal are due to random errors in the A and B channels, which are associated with counting. Note that this test cannot be performed when the reagent gas is pulsed, since even with the plasma off, there is a signal difference between the two channels.

In both methods, the pulsing rate is critical to the reduction of error due to any drift in the experiment, since (*A*) is counted after (*B*). If the pulse valve is operated slowly, any drift in the system creates larger errors in the signal (A–B), because there is a greater time difference between measurements of *A* and of *B*. Thus a faster pulse rate eliminates some of the effects of instabilities in the plasma. Studies with small and larger drifts have shown that this is indeed the case, however, every effort is made to minimize drift by servo controlling the flows of the gases added to the flow tube.

Finally, the sensitivity of detection (i.e., detection of a small signal in a large background) was quantified by using a constant large flow of CH_4, which simulates a large background, the small modulated signal being emulated by pulsing in ~0.20% of CH_4 in a mix with He. CH_4^+ was used as the monitor ion. By doing this, it was found that for a 50 s counting period the limit of detection is at least $\sim 10^{-3}$ signal to background, see Fig. 6. In this experiment, the DR product that typically has the highest background is the one that is the same as the reagent gas that is used, thus detecting the other products should be less of a problem since their associated background is lower. For example, in the case of DR of N_2H^+, the DR product N_2 has the highest background, whereas mass 15, measured for NH has nearly no background.

3.2. N_2H^+ recombination

The details of the analysis for this DR can be found in Molek et al. [39] and only the features that illustrate the technique will be covered here. Note that the He throughput used for the study of N_2H^+ was 31.4 slm to decrease the residence time in the flow tube, thus reducing any effects due to diffusion of DR products. The experiment was repeated at 16.0 slm for comparison and it was found that no change was observed in the product distribution as expected if the relative diffusive loss is small for both flows. Data presented in this paper, for the electron attaching gas method, was collect at a throughput of 16.0 slm.

The two methods have been used in this DR. It should be noted that there are very small N_2 impurities in the He buffer gas but because these are constant in the flow tube they do not contribute to the signals, see Eq. (9). Here the products N_2, NH, and N have the respective monitor ions, N_2^+, NH^+, and N^+, which are characterized after electron impact ionization and mass spectrometric detection and identification. Note that when the attaching gas is pulsed in, there is the possibility for ion–ion recombination (iir) to take place. Below are the possible products from the iir reaction between N_2H^+ and Cl^-.

$$N_2H^+ + Cl^- \rightarrow N_2H + Cl + 511\,kJ/mol\,(5.3\,eV) \quad (11)$$

$$N_2H^+ + Cl^- \rightarrow N_2 + H + Cl + 473\,kJ/mol\,(4.9\,eV) \quad (12)$$

$$N_2H^+ + Cl^- \rightarrow N_2 + HCl + 897\,kJ/mol\,(9.3\,eV) \quad (13)$$

$$N_2H^+ + Cl^- \rightarrow NH + NCl + 203\,kJ/mol\,(2.1\,eV) \quad (14)$$

$$N_2H^+ + Cl^- \rightarrow NH + N + Cl - 135\,kJ/mol\,(1.4\,eV) \quad (15)$$

This can produce a small error in the calculation of the DR products, where a product from iir will make a DR product at the same mass appear smaller. However, based on the difference in rate coefficients between these processes, in which iir is typically about an order of magnitude slower [40], and assuming a worst case condition that only one product channel of iir is generated, say channel (14), then the maximum error in the NH DR product is less than 10%. If the NH product from DR were >10% then it would be detectable, but appear to be smaller than it really is. If the DR product NH were 10% then the DR signal from this product would appear to be zero. However, here the signal from the NCl product, which would be produced in parallel with NH (see Eq. (14)), would be detectable and negative since it can only result from iir. With this in mind, the possible products unique to iir were followed using the monitor ions Cl^+, HCl^+, and NCl^+, thus covering all possible product channels, see Fig. 7. From this it can be seen that products from the iir are almost non-existent, with Cl^+, NCl^+, and HCl^+ oscillating near zero, therefore establishing that the effects of iir are indeed very small and implying that this is a slow recombination. The study of this reaction shows that iir is not affecting the DR product distribution in this case. The results for DR of N_2H^+ show $N_2 + H$ to be very dominant; the observed N^+, see Fig. 7a, is from N_2 fragmentation by electron impact and not from NH + N products. This is very different from the SR data [24]. To further ensure that iir is not affecting the product distribution and to corroborate these results, the second method was used. Briefly, the reagent gas, N_2, was pulsed in to form the recombining ion, in this case N_2H^+ where the difference between N_2 in (*A*) versus N_2 out (*B*) is the signal, Eq. (9). There are two possible contributors to this signal, one is a fraction of unreacted reagent gas (f_1) and the other is a product of DR (f_2). In the experiment, the contribution of f_1 to the total signal needs to be minimized while maximizing f_2 contribution. This is achieved by reducing the initial concentration of N_2, such that the range between the lowest and highest concentrations encompasses the electron density ($[e] = \sim 3.0 \times 10^{10}$ molecules/cm^3) just downstream of the pulse addition point. This is critical because as $[N_2]$ is reduced, the signal changes from the observed electron impact fragmentation of N_2 to a signal that is a mixture of the products of DR and electron impact fragmentation of N_2. Here, the DR product

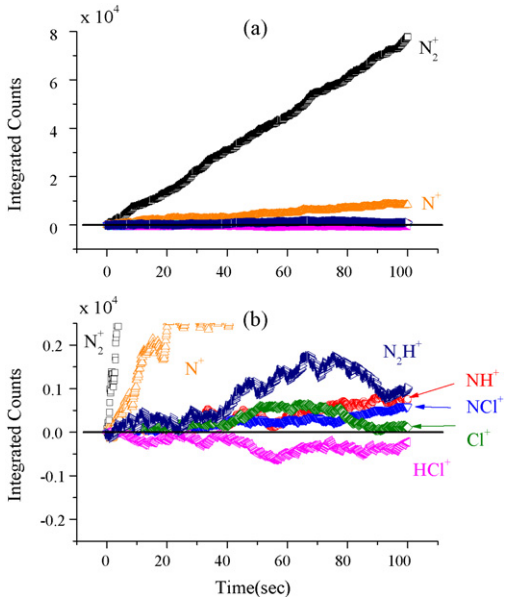

Fig. 7. Integrated monitor ion signals for DR of N_2H^+. Shown is the integrated signal from all the monitored species, for both DR and iir products. It can be clearly seen (a) that the biggest signal build up is from the N_2^+ monitor ion. The next largest signal is from N^+, which is solely due to the electron impact ionization and fragmentation of N_2. The (b) plot, is an expanded scale (about ×35) of counts, around the zero, for the other products. It shows that the NH^+ monitor signal of NH is very small (~2%). The products that can originate only from iir are also very small showing that little iir is occurring.

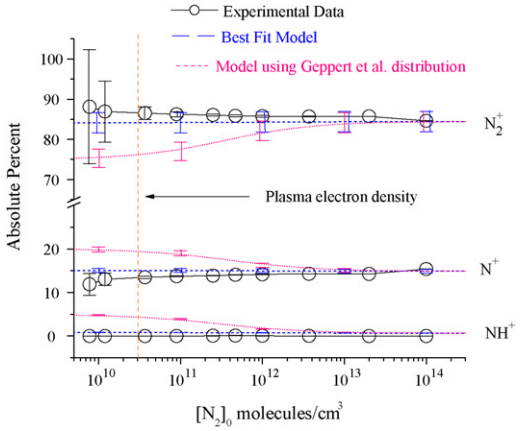

Fig. 8. Absolute ion percentages of the monitor ions, in both model and experiment, as a function of initial N_2 concentration. The solid lines with open circles (black) represent the experimental data. The blue dashed and pink dotted lines represent the kinetic model results using two different values for the absolute DR product percentages. The pink dotted line uses Geppert et al. results [24], N_2 (36%) and NH (64%), and the blue dashed lines are the models best fit which uses N_2 (98%) and NH (2%). The best fit model agrees with the experimental data far better than the model using Geppert et al. results. In addition, error bars are included on the experimental data and estimates of the error on the model; see Section 3.5 for details. (For interpretation of the references to color in this figure legend, the reader is referred to the web version of the article.).

contribution to the overall detected signal would be at a maximum with $[N_2H^+] \approx [+] \approx [e] \approx 3.0 \times 10^{10}$ molecules/cm^3. Therefore, DR products must be $\leq [e^-]$ and this limits the contribution of DR products (f_2) to the total signal. At high $[N_2]$ concentrations ($\sim 1 \times 10^{14}$ molecules/cm^3), the fraction of unreacted reagent gas dominates over the DR products by nearly 4 orders of magnitude, therefore a plot of the absolute percent of each monitor ion, in this case N_2^+, NH^+, and N^+(i.e., monitors for N_2, NH, and N), versus $[N_2] = 1 \times 10^{14}$ molecules/cm^3 results in the electron impact fragmentation pattern of N_2. As the $[N_2]$ concentration approaches $[e^-]$, the fraction of unreacted reagent gas decreases and the products from DR contribute more significantly to the overall signal. This leads to a deviation from the electron impact fragmentation pattern of N_2. The modeling of this situation is shown in Fig. 8. Inherent in the pulsing technique is that any impurity in the flow tube is a constant background, which gets subtracted out. This is especially important in the pulsed reagent gas method, since it enables N_2 products to be detected at the low $[N_2]$ concentrations needed to observe the deviation from the fragmentation pattern. It should be noted that the data point at the lowest $[N_2]$ concentration is difficult to obtain with an error of <10% in the final product distribution in a reasonable amount of time. This is because the $[N_2]$ is small and thus the degree of reaction is small. The final DR distributions from the two methods are shown in Table 4.

An exhaustive effort was made during these experiments to reconcile the difference between the current FA measurements and SR measurements of Geppert et al. [24]. In particular, possible errors

Table 4
Present values of the products for DR of N_2H^+. The literature SR value is shown for comparison. Method 1 uses pulsing of CCl_4 and method 2 pulsing of N_2.

	FA [39]		SR [24]
	Method 1	Method 2	
$N_2H^+ + e^- \rightarrow N_2 + H$	95–100%	95–100%	36%
$N_2H^+ + e^- \rightarrow NH + N$	0–5%	0–5%	64%

in the FA study have been analyzed in great detail. For the SR, it is known that there were contamination issues due to $^{14}N^{15}N^+$ in the ring; this would DR into $^{14}N + {}^{15}N$, where the ^{15}N would appear like a ^{14}NH product. It should be noted that due to our measurements, the SR experiment was repeated and indeed it was shown that this was the reason for the discrepancy and that the NH channel was about 10% [9], consistent with the FA result. This illustrates the importance of measuring DR product distributions with more than one technique.

Also, the ion source in the SR study is a hot filament ion source that operates at temperatures over 1000 K [41]. N_2 ionizes 3 times more efficiently than H_2 for the experimental conditions [24] and thus to produce N_2H^+ for injection into the ring it relies on the reaction,

$$^{14}N^{14}N^+ + H_2 \rightarrow {}^{14}N^{14}NH^+ + H \quad (16)$$

It should be noted that Geppert et al. quote a room temperature rate coefficient for reaction (16), but there is experimental evidence for similar reactions showing that the rate constants tend to decrease as the temperature increases [76].

3.3. CH_5^+ recombination

This recombination is particularly relevant to the interstellar medium since CH_5^+ DR was thought to be a source of CH_4 [42], until storage ring measurements showed CH_3 (~75%) as a dominant product from this recombination [16]. This removed CH_5^+ DR as the source of methane in interstellar clouds [42]. In the DR recombination of CH_5^+, the energetically accessible pathways are,

$$CH_5^+ + e^- \rightarrow CH_4 + H + 769\,\text{kJ/mol}\,(8.0\,\text{eV}) \quad (17)$$

$$CH_5^+ + e^- \rightarrow CH_3 + H_2 + 766\,\text{kJ/mol}\,(7.9\,\text{eV}) \quad (18)$$

$$CH_5^+ + e^- \rightarrow CH_3 + 2H + 330\,\text{kJ/mol}\,(3.4\,\text{eV}) \quad (19)$$

$$CH_5^+ + e^- \rightarrow CH_2 + H_2 + H + 307\,\text{kJ/mol}\,(3.2\,\text{eV}) \quad (20)$$

$$CH_5^+ + e^- \rightarrow CH + 2H_2 + 317\,\text{kJ/mol}\,(3.3\,\text{eV}) \quad (21)$$

Since the attaching gas method is an extremely effective way to determine the products of DR; efforts have been concentrated

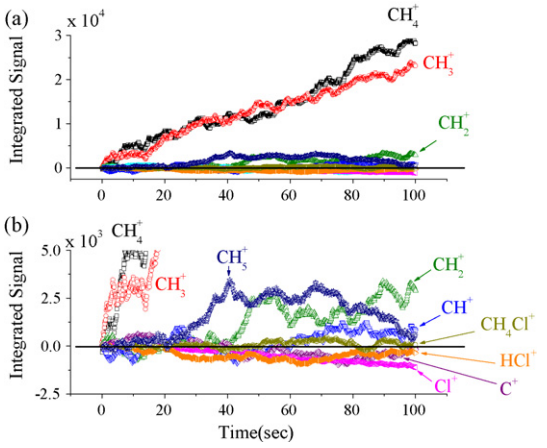

Fig. 9. The integrated signal build-up of all the monitored species, for both DR and iir products of CH_5^+ recombination is shown. In (a), it can be clearly seen that the biggest signals are from CH_4^+ and CH_3^+ monitor ions. The majority of the CH_3^+ signal is from the electron ionization and fragmentation of CH_4, see Table 3. The plot in (b) is an enlarged scale, around the zero, to distinguish the other products. There is a small negative build up of Cl^+ and possibly HCl^+, products of iir, however, these are very small; see text for further discussion.

on this approach. The experiments show a large build up of the CH_4^+ signal, a monitor ion for CH_4. This signal is due to the DR product of CH_4 and not the unreacted CH_4 reactant gas in the flow tube. This is reinforced by two experimental examples. The first is shown in Fig. 5 and was discussed in detail in the text, see Section 3.1. It demonstrates the ability to integrate and show that there is ~0 signal even when there is a large background (3×10^5 counts/s) of CH_4; thus unreacted background is not contributing to signal build up. The second example is discussed in detail in Molek et al. [39]. Briefly, two DR systems were studied with recombining ions HCO^+ and CO^+, while one monitor ion (CO^+ for CO DR product) was used. Since the CO^+ recombining ion can only dissociate upon DR (i.e., no product CO), the CO^+ monitor should integrate around the zero for this recombination. However, in the case of HCO^+ DR, CO is a major product (92%) [43] and therefore an integrated signal of the CO^+ monitor should be very evident. Fig. 5 in Molek et al. [39] shows that for HCO^+ DR, the CO^+ monitor ion builds up over time corresponding to a CO product. However in the CO^+ DR case, the CO^+ monitor ion oscillates around the zero with time integrating out a large background. This is expected since CO is not a product from this recombination. Therefore, there is no erroneous build up of signal in the FA experiments and background effects are shown to be eliminated.

The experimental conditions for DR study of CH_5^+ are those listed in Section 2.2. The build up of CH_4^+ and CH_3^+ monitor ions can readily be seen in Fig. 9a. Note that CH_3^+ is a major ion fragment of electron impact ionization of CH_4 [34], thus the CH_3^+ integrated ion signal is nearly all attributable to the fragmentation contribution of electron impact ionization of the DR product CH_4. The plot in Fig. 9b shows the monitor ions for CH_2^+ and CH^+ as well as the monitor ions for some of the energetically possible iir products, where the energetically accessible channels are

$$CH_5^+ + Cl^- \rightarrow CH_4 + HCl + 856\,kJ/mol\,(8.9\,eV) \quad (22)$$

$$CH_5^+ + Cl^- \rightarrow CH_4 + H + Cl + 424\,kJ/mol\,(4.4\,eV) \quad (23)$$

$$CH_5^+ + Cl^- \rightarrow CH_3 + H_2 + Cl + 424\,kJ/mol\,(4.4\,eV) \quad (24)$$

$$CH_5^+ + Cl^- \rightarrow CH_3Cl + H_2 + 773\,kJ/mol\,(8.0\,eV) \quad (25)$$

$$CH_5^+ + Cl^- \rightarrow CH_3 + H + HCl + 424\,kJ/mol\,(4.4\,eV) \quad (26)$$

$$CH_5^+ + Cl^- \rightarrow CH_3Cl + 2H + 341\,kJ/mol\,(3.5\,eV) \quad (27)$$

Table 5
Product distributions for CH_5^+ recombination. Results of the current work are shown in comparison to SR data.

		FA (this work)	SR[16]
$CH_5^+ + e^-$	$\rightarrow CH_4 + H$ (17)	95% ±5%	4.9 ± 1.3%
	$\rightarrow CH_3 + H_2$ (18)	≤ 8%	4.8 ± 0.2%
	$\rightarrow CH_3 + 2H$ (19)		69.8% ± 0.8%
	$\rightarrow CH_2 + H + H_2$ (20)	≤ 1%	17.2% ± 1.6%
	$\rightarrow CH + H_2 + H_2$ (21)	≤ 1%	3.3 ± 1.1%

$$CH_5^+ + Cl^- \rightarrow CH_2 + H_2 + HCl + 390\,kJ/mol\,(4.0\,eV) \quad (28)$$

$$CH_5^+ + Cl^- \rightarrow CH_2Cl + H_2 + H + 354\,kJ/mol\,(3.7\,eV) \quad (29)$$

$$CH_5^+ + Cl^- \rightarrow CHCl + 2H_2 + *\,kJ/mol \quad (30)$$

It should be noted that it is very difficult to monitor the H_2^+ and H^+ ions since they are at a very low mass for the quadrupole mass filter. This results in difficulties getting quantitative values for these products. However, there are enough monitor ions to quantify all possible channels except the two CH_3Cl channels and yet this was not a problem since CH_3Cl^+ was not a detectable signal (not shown in Fig. 9b). Notice that there is a small negative build up of the Cl^+. This product is small (<2%) but still indicates that some iir is taken place. In the case of Cl^+, the presence of CCl_3 may contribute to some of the negative build up by ionization of the CCl_3. As far as the authors are aware the fragmentation pattern of CCl_3 is not available in the literature, thus the Cl^+ contribution from this source cannot be assessed in detail. However, in the N_2H^+ recombination, Cl^+ is not observed and this is for similar experimental conditions, thus implying that CCl_3 does not fragment significantly to Cl^+ on electron impact. This is an indicator that Cl is a product of iir of CH_5^+, which suggests a general way of determining the products of iir. Here the conditions would then be optimized for iir recombination rather than DR. Note that electron impact ionization of CCl_4 cannot be a source of Cl^+ since all of this is destroyed in the electron attachment process. To the author's knowledge, this is the first data on the products of iir for $CH_5^+ + Cl^-$. The CH_5^+ DR product distribution determined in the present study is shown in Table 5 together with the SR data from Semaniak et al. [16]. The dominant product in the FA measurement, CH_4, is in stark contrast to the SR data where the dominant product is CH_3. The reasons for this difference are not understood at present and need more investigation in both the FA and SR. Some additional information is available from a study by Adams et al. [13] in which the total H-atom fraction was determined for a series of DR including CH_5^+. Here the fraction was 1.18 and is equivalent to (17) + 2(19) + (20) where the equation numbers for the individual channels are given in parenthesis, see also in Table 5. The present FA data for this gives two limits ≤1.03 and ≤1.11 depending on whether Eqs. (18) or (19) is dominant and is in good agreement, whereas the SR value of 1.58 is very different.

3.4. Calculation of the DR product distribution

The determination of the product distribution from the measured counts in the FA are complex but relatively straightforward. For example, the DR of an ion, with the formula H_3X^+, has three possible DR product channels: H_2X, HX, and X,

$$H_3X^+ + e^- \rightarrow H_2X + H\,x_1 \quad (31)$$

$$H_3X^+ + e^- \rightarrow HX + H_2(2H)\,x_2 \quad (32)$$

$$H_3X^+ + e^- \rightarrow X + H_2(2H) + H \quad x_3 \tag{33}$$

where each of these product channels contribute a fraction (x_1, x_2, and x_3) to the total number of neutral DR products (N) i.e., the number of recombinations. Each of the neutral products, when ionized by 70 eV electrons, may non-dissociatively ionize or dissociatively ionize where the amount of each ion produced is dictated by the product of the total cross section ($\sim\sigma_{Tm}$) and absolute fraction (d_{mn}) for that particular ionization pathway, e.g.,

$$H_2X(x_1N) \xrightarrow{e^-(70\,eV)} H_2X^+(\sigma_{T2}d_{22}) \tag{34}$$

$$H_2X(x_1N) \xrightarrow{e^-(70\,eV)} HX^+(\sigma_{T2}d_{21}) \tag{35}$$

$$H_2X(x_1N) \xrightarrow{e^-(70\,eV)} X^+(\sigma_{T2}d_{20}) \tag{36}$$

The notation for the absolute fraction is represented as, m being the number of H's in the product neutral and n the number of H's in the monitor ion produced by electron impact. For example, d_{21} is the fraction of HX^+ coming from the H_2X product neutral. The rest of the DR products follow the same logic.

$$HX(x_2N) \xrightarrow{e^-(70\,eV)} HX^+(\sigma_{T1}d_{11}) \tag{37}$$

$$HX(x_2N) \xrightarrow{e^-(70\,eV)} X^+(\sigma_{T1}d_{10}) \tag{38}$$

$$X(x_3N) \xrightarrow{e^-(70\,eV)} X^+(\sigma_{T0}d_{00}) \tag{39}$$

Note that the total cross sections, σ_{Tm}, correct for the difference in ionization efficiency for each of the DR products. To calculate the monitor ion signals that should be detected, the different contributors to each ion must be summed together. Starting with H_2X^+ (this is the largest mass so there is only one contributing term)

$$\{H_2X^+\}_{detected} = x_1N\sigma_{T2}d_{22} \tag{40}$$

where x_1N is the fractional contribution of H_2X to the DR product distribution and $\{H_2X^+\}_{detected}$ represents the total number of H_2X^+ monitor ions detected. The signal from the smaller ions also have the additional contribution from the larger species represented below, viz

$$\{HX^+\}_{detected} = x_2N\sigma_{T1}d_{11} + \underbrace{x_1N\sigma_{T2}d_{21}}_{(d_{21}/d_{22}\{H_2X^+\}_{detected})} \tag{41}$$

$$\{X^+\}_{detected} = x_3N\sigma_{T0}d_{00} + \overbrace{x_2N\sigma_{T1}d_{10}}^{(d_{10}/d_{11}[\{HX^+\}_{detected} - d_{21}/d_{22}\{H_2X^+\}_{detected}])} + \underbrace{x_1N\sigma_{T2}d_{20}}_{(d_{20}/d_{22}\{H_2X^+\}_{detected})} \tag{42}$$

The equations can be rearranged to solve for x_1, x_2, and x_3 giving,

$$x_1N = \frac{\{H_2X^+\}_{detected}}{\sigma_{T2}d_{22}} \tag{43}$$

$$x_2N = \frac{(\{HX^+\}_{detected} - d_{21}/d_{22}\{H_2X^+\}_{detected})}{\sigma_{T1}d_{11}} \tag{44}$$

$$x_3N = \frac{\{X^+\}_{detected} - d_{20}/d_{22}\{H_2X^+\}_{detected} - d_{10}/d_{11}[\{HX^+\}_{detected} - d_{21}/d_{22}\{H_2X^+\}_{detected}]}{\sigma_{T0}d_{00}} \tag{45}$$

Note that N is an absolute number of recombinations which we do not know, but only relative fractions are needed so this is of no significance. Thus, if the σ and d and the monitor ion signals are known, the product distribution can be determined.

Table 6
Modeled losses of neutral products in the FA relative to a starting distribution using the Semaniak et al. [16] product distribution. Listed are the products and the distribution from the model with considerations for diffusion of radicals (CH_3, CH_2, and CH) and neutral-neutral reactions (46)–(49). For comparison, the distribution obtained by Semaniak et al. [16] is included.

	Model results using Semaniak et al. [16] data	
	Distribution (Semaniak)	Distribution (Molek)
CH_4	4.9%	7.1%
CH_3	74.6%	73.3%
CH_2	17.2%	18.6%
CH	3.3%	0.95%

3.5. Sources of error

The possible sources of error in our measurements that need to be explored are (i) the ion–ion recombination effect, (ii) DR product loss due to neutral–neutral reactions, and (iii) neutral diffusive loss. These sources of error have been discussed for the N_2H^+ recombination by Molek et al. [39]. For CH_5^+ recombination, the iir product channels that would take away from the CH_3 DR product are channels (24) and (26). Even in the worst case situation with the observed Cl^+ and HCl^+ products only coming from channels (24) and (26) and not the others (i.e., (22), (23), and (28)) then the CH_3 product would only increase ~2%, which does not explain the large discrepancy with the SR. The remaining loss processes are diffusive loss and neutral–neutral reactive loss of the radical neutrals. Note, it is assumed in this model that the radical species will diffuse to the walls of the flow tube and then be 100% lost by reactions with other available neutrals. Of all the possible neutral–neutral reactions that would deplete the DR products, only four have an effect on the distribution, these being:

$$CH_3 + CH_3 \rightarrow C_2H_5 + H \quad k = 4.6 \times 10^{-11}\ cm^3\ s^{-1}\ [44] \tag{46}$$

$$CH_3 + CH_2 \rightarrow C_2H_4 + H \quad k = 2.1 \times 10^{-10}\ cm^3\ s^{-1}\ [44] \tag{47}$$

and

$$CH + H_2 \rightarrow CH_2 + H \quad k = 2.3 \times 10^{-12}\ cm^3\ s^{-1}\ [45] \tag{48}$$

$$CH + CH_4 \rightarrow Products \quad k = 5.4 \times 10^{-11}\ cm^3\ s^{-1}\ [46] \tag{49}$$

The Semaniak et al. [16] distribution is used as a starting point to gauge how these losses (ii and iii) in the FA experiment would affect the distribution. It can be seen in Table 6 that the effects of these losses are only a few percent, even for the worst case conditions. Even so, these are taken into account in the error figures associated with the product distribution. This again is not enough to explain the discrepancy between the current FA measurements and those in the SR. Every effort has been made to account for any losses in the product channels for the FA.

3.6. Errors in the product distributions

To evaluate the overall errors in the FA product distributions considered here, a detailed error analysis has been performed for each case. The majority of the error in the distributions is associated with the random error inherent in counting statistics, where errors in channels A and B are the square roots of the number of counts in A and B, respectively. The error associated with the signal is then

$$\sigma_S = \sqrt{A + B} \tag{50}$$

see reference [47] for details. Additionally but with less significance, is the error associated with the electron impact fragmentation patterns (d_{mn}) and ionization cross sections (σ_{Tm}). Again these have been evaluated for each DR study. All of these errors were considered for both the N_2H^+ and CH_5^+ DR systems, thus giving the upper limit error for the various products, see Tables 4 and 5.

A further effect has to be considered if any of the recombination products are produced in excited states (an example of this is the production of the N_2 ($B^3\Pi_g$) state in the DR of N_2H^+). What the FA determines is the product distribution at the electron impact ionizer. Thus any excited state products with a short radiative lifetime (≪than the 5 ms residence time in the flow tube before detection) will have decayed. This is readily achieved for allowed electronic transitions for which the radiative lifetimes are $\sim 10^{-9}$ s. Note that collisional relaxation can also occur with gases present in the flow tube, especially for vibrational deexcitation. Thus, here the total neutral product distribution will be obtained. This would be directly comparable with SR data where the neutral products are detected in high velocity collisions (∼MeV) with the energy detector which would not be sensitive to internal product energy. In the FA, if metastable states are produced in DR and these reach the detector then the σ_{Tm} and d_{mn} could be different from those for the ground state. A case in point is the production of the N_2 ($B^3\Pi_g$) as an 19% product of the N_2H^+ DR [48]. This has a radiative lifetime of 8 μs [49], and thus will have decayed before reaching the detector. However, this decay is to the electronically excited N_2 ($A^3\Sigma_u^+$), state which has a radiative lifetime of 1.3 s [49] and would reach the detector if not collisionally relaxed. If this occurs, then with the internal energy (up to 6.66 eV), the electron impact fragmentation would be expected to be different from the ground state. Yet, the absolute observed fragmentation to N^+ of 10.3% (see Fig. 7) is consistent with the NIST value (15%) for the ground state [34] and our value (11.1%) for N_2 added to the flow tube without a discharge and thus all ground state. This implies that collisional relaxation does indeed occur. The presence of excited states in the DR of N_2H^+ was detected spectroscopically [51].

In the case of CH_5^+ DR, no electronically excited states of CH_4 (Eq. (17)) are accessible. Rovibronic excitation is possible but this would be expected to be rapidly quenched by collisions with CH_4 and He in the flow tube before the detection system. However, if there is a large amount of rovibronic excitation, it is possible that $CH_4^* \rightarrow CH_3 + H$ could be accessible and occur on a time scale of a vibrational period ($\sim 10^{-14}$ s). It is not known how much vibrational excitation remains in the CH_4^*, since the amount of kinetic energy used in the initial $CH_4^* + H$ dissociation is not known. But the time scale of the vibrational period is shorter than both the He collision time in the FA ($\sim 10^{-7}$ s) and the time to get from the recombination region to the detector in the SR ($\sim 10^{-6}$ s) and thus any predissociation of the CH_4^* would occur in both the FA and SR. That it does not occur in the FA implies that there is no production of CH_3 by this mechanism and a different solution needs to be sought. For the $CH_3 + 2H$ channel (Eq. (19)), no electronically excited states are again accessible, however, such can be reached in the $CH_3 + H_2$ channel (Eq. (18)), viz, 3 s $^2A_1'$ and 3p $^2A_2''$ [52] which could possibly radiate to the ground $X\,^2A_2''$ state [53], although the 3 s state predissociates $CH_2 + H$ [54]. None of the emissions were observed in spectral scans from 180 to 800 nm. In addition, if excited CH_3 survived to the detection system, more electron impact ionization to CH_2^+ and CH^+ would be expected. Very little CH_2^+ (≤1%) and CH (≤1%) were observed indicating little production of excited CH_3. Also, since the CH and CH_2 contributions to the product distribution are so small, the fact that they can be produced in electronically excited states is of no consequence. Note that, the measurements of the CH_3 radical fragmentation pattern, Table 3, were done by electron attachment of CH_3I to form CH_3. This electron attachment process has ∼0.59 eV of excess energy, which is not enough to electronically excite CH_3; thus this is not affecting the fragmentation pattern.

4. Conclusions

A new technique has been developed to quantitatively determine the neutral products of dissociative electron-ion recombination, DR. It has been shown that this technique is immensely valuable for this purpose. As it stands, there are several discrepancies in the literature between the SR and previous spectroscopic measurements; this new technique may give a better understanding of the reasons for the differences. As a case in point, for the N_2H^+ recombination, the SR results have been re-measured showing that the NH product is not nearly as important as originally thought [9]. For the CH_5^+ recombination, all possible sources of error have been evaluated for the new FA technique, yet the discrepancies with the SR have not been reconciled. It is interesting to note that the $CH_4 + H$ channel is supported by Bates' theoretical suggestions for this DR [55]. In addition, Mann et al. [56] have used dissociative charge exchange between CH_5^+ and Cs to generate highly excited CH_5. They found that dissociation to form $H + CH_4$ was favored over $H_2 + CH_3$ in a ratio of 14:1 consistent with the value of 12:1 for the present data and consistent with theory (Bowman, Priv. Com. 2007). These are at variance with the SR value of 0.03:1. It should also be noted that the present study gave an H-atom fraction in the range 0.96–1.12 close to the values of 1.16 and 1.19 determined in our earlier FA studies using vuv absorption [13], but substantially smaller than the SR value of 1.58 [16]. It is critical to resolve the differences since DR of CH_5^+ forming CH_4 could be a very important source of methane in the ISM [42].

In the SR, evidence for the possible vibrational excitation in the recombining CH_5^+ ion has been suggest by Sheehan and St.-Maurice [57]. In a merged beam study, the recombination rate constant was measure as a function of temperature ($k = 2.9 \times 10^{-7}$ cm^3 s^{-1} with a temperature dependence of $T^{-0.46}$) and is very consistent with the SR results ($k = 2.8 \times 10^{-7}$ cm^3 s^{-1} with a temperature dependence of $T^{-0.52}$) [16]. Note that the room temperature SR rate constant is a factor of 2.5–5.0 below the FA values [58–61]. In the Sheehan study, it was known that there was vibrational excitation in the recombining ions and they suggested, on the basis of the agreement, that the SR results may have vibrational excitation in the ion. This is consistent with reports from the SR that the ion source used in the experiment produces vibrationally excited molecular ions [41]. However, such excitation is reported as being vibrationally relaxed with multiple passes around the ring [62]. Another possibility may include residual rotational excitation in the recombining ion where the SR has no mechanism to quench all this excess energy. It was seen in H_3^+ DR that recombination rate varied as a function of vibrational/rotational energy [63]. Other important studies include H_3O^+ DR, in which disagreement still exists. Due to their relevance to the ISM and Titan's atmosphere, other ions of particular interest are NH_4^+, $CH_3OH_2^+$, and $CH_3OCH_4^+$ [22,64]. In addition to these room temperature studies, there is the possibility of investigating the temperature dependence of product distributions. Lastly, experimental conditions in the FA can easily be changed to enhance ion–ion recombination and providing a means of studying its products. The products formed can give insight into the mechanism that is occurring, be it a long range charge transfer or an intimate encounter pathway [65–67]. This will give further experimental insight into the mechanism of this process, which has been long considered as a long range electron transfer [40].

Acknowledgements

Funding under NSF Grant No. 0212368 is gratefully acknowledged.

References

[1] E. Herbst, in: T.J. Millar, D.A. Williams (Eds.), Rate Coefficients in Astrochemistry, Kluwer, Dordrecht, 1988, pp. 239–262.
[2] T.E. Cravens, in: S.L. Guberman (Ed.), Dissociative Recombination of Molecular Ions with Electrons, Kluwer, New York, 2003, pp. 385–400.

[3] P. Eberhardt, M. Reber, D. Krankowsky, R.R. Hodges, Astron. Astrophys. 302 (1995) 301–316.
[4] J.L. Fox, in: B.R. Rowe, J.B.A. Mitchell, A. Canosa (Eds.), Dissociative Recombination Theory, Experiment and Applications II, Plenum, New York, 1993, p. 219.
[5] J.M. Goodings, N.S. Karellas, C.S. Hasanali, Int. J. Mass Spectrom. Ion Proc 89 (1989) 205–226.
[6] N.G. Adams, L.M. Babcock, J.L. McLain, in: P. Armentrout (Ed.), Encyclopedia of Mass Spectrometry: Theory and Ion Chemistry, vol. 1, Elsevier, Amsterdam, 2003, pp. 542–555.
[7] N.G. Adams, V. Poterya, L.M. Babcock, Mass Spectrom. Rev. 25 (2006) 798–828.
[8] A.I. Florescu-Mitchell, J.B.A. Mitchell, Phys. Rep.-Rev. Section Phys. Lett. 430 (2006) 277–374.
[9] W.D. Geppert, M. Larsson, Mol. Phys. 106 (2008) 2199–2226.
[10] M. Larsson, A.E. Orel, Dissociative Recombination of Molecular Ions, 1st ed., Cambridge University Press, Cambridge, UK, 2008.
[11] B.R. Rowe, J.L. Queffelec, in: J.B.A. Mitchell, S.L. Guberman (Eds.), Dissociative Recombination: Theory, Experiment and Applications, World Scientific, Singapore, 1989, pp. 151–161.
[12] C.R. Herd, N.G. Adams, D. Smith, Ap. J. 349 (1990) 388–392.
[13] N.G. Adams, C.R. Herd, M. Geoghegan, D. Smith, A. Canosa, J.C. Gomet, B.R. Rowe, J.L. Queffelec, M. Morlais, J. Chem. Phys. 94 (1991) 4852–4857.
[14] N.G. Adams, C.R. Herd, D. Smith, J. Chem. Phys. 91 (1989) 963–973.
[15] T.L. Williams, N.G. Adams, L.M. Babcock, C.R. Herd, M. Geoghegan, Mon. Not. Roy. Astr. Soc. 282 (1996) 413–420.
[16] J. Semaniak, A. Larson, A. Le Padellec, C. Stromholm, M. Larsson, S. Rosen, R. Peverall, H. Danared, N. Djuric, G.H. Dunn, S. Datz, Ap. J. 498 (1998) 886–895.
[17] Z. Amitay, D. Zaijman, P. Forck, U. Hechtfischer, B. Seidel, M. Grieser, D. Habs, R. Repnow, D. Schwalm, A. Wolf, Phys. Rev. A 54 (1996) 4032–4050.
[18] V. Kokoouline, C.H. Greene, J. Phys.: Conf. Ser. 4 (2005) 74–82.
[19] A. Lampert, A. Wolf, D. Habs, J. Kenntner, G. Kilgus, D. Schwalm, M.S. Pindzola, N.R. Badnell, Phys. Rev. A 53 (1996) 1413–1423.
[20] S.L. Guberman, J. Phys.: Conf. Ser. 4 (2005) 58–65.
[21] J.H. Waite, H. Nieman, R.V. Yelle, W.T. Kasprzak, T.E. Cravens, J.G. Luhmann, R.L. McNutt, W.-H. Ip, D. Gell, V. de la Haye, I. Muller-Wordag, B. Magee, N. Borggren, S. Ledvina, G. Fletcher, E. Walter, R. Miller, S. Scherer, R. Thorpe, J. Xu, B. Block, K. Arnett, Science 308 (2005) 982–986.
[22] T.E. Cravens, I.P. Robertson, J.H. Waite, R.V. Yelle, W.T. Kasprzak, C.N. Keller, S.A. Ledvina, H.B. Nieman, J.G. Luhmann, R.L. McNutt, W.-H. Ip, V. de la Haye, I. Mueller-Wodarg, J.-E. Wahlund, V.G. Anicich, V. Vuitton, Geophys. Res. Lett. 33 (2006) L07105.
[23] A. Ehlerding, F. Hellberg, R. Thomas, S. Kalhori, A.A. Viggiano, S.T. Arnold, M. Larsson, M.A. Ugglas, Phys. Chem. Chem. Phys. 6 (2004) 949–954.
[24] W. Geppert, R. Thomas, J. Semaniak, A. Ehlerding, T.J. Millar, F. Osterdahl, M.af Ugglas, N. Djuric, A. Paal, M. Larsson, Ap. J. 609 (2004) 459.
[25] W. Geppert, R. Thomas, A. Ehlerding, F. Hellberg, F. Osterdahl, M.A. Ugglas, M. Larsson, Int. J. Mass Spectrom. 237 (2004) 25–32.
[26] J.B.A. Mitchell, C. Rebrion-Rowe, J.L. Le Garrec, G. Angelova, H. Bluhme, K. Seiersen, L.H. Andersen, Int. J. Mass Spectrom. 227 (2003) 273–279.
[27] F. Vallee, J.C. Gomet, B.R. Rowe, J.L. Queffelec, M. Morlais, in: M.S. Varda, S.P. Tarafdar (Eds.), Astrochemistry, Kluwer, Dordrecht, 1987, pp. 29–30.
[28] E. Alge, N.G. Adams, D. Smith, J. Phys. B 16 (1983) 1433–1444.
[29] D. Smith, N.G. Adams, in: F. Brouillard, J.W. McGowan (Eds.), Physics of Ion–Ion and Ion-Electron Collisions, Plenum Press, New York, 1983, pp. 501–531.
[30] V. Anicich, An Index of the Literature for Bimolecular Gas Phase Cation-Molecule Reaction Kinetics, JPL Publication 03-19, Jet Propulsion Laboratory, Pasadena, 2003.
[31] Y. Ikezoe, S. Matsuoka, M. Takebe, A.A. Viggiano, Gas Phase Ion-Molecule Reaction Rate Constants through 1986, Ion Reaction Research Group of the Mass Spectroscopy Society of Japan, Tokyo, 1987.
[32] T.L. Williams, B.K. Decker, N.G. Adams, L.M. Babcock, P.W. Harland, Rev. Sci. Instrum. 71 (2000) 2169–2179.
[33] T. Mostefaoui, N.G. Adams, L.M. Babcock, Rev. Sci. Instrum. 73 (2002) 2044–2050.
[34] P.J. Linstrom, W.G. Mallard (Eds.), NIST Chemistry WebBook, National Institute of Standards and Technology, Gaithersburg MD, 20899, June 2005.
[35] F.A. Baiocchi, R.C. Wetzel, R.S. Freund, Phys. Rev. Lett. 53 (1984) 771–774.
[36] V. Tarnovsky, A. Levin, H. Deutsch, K. Becker, J. Phys. B-Atomic Mol. Opt. Phys. 29 (1996) 139–152.
[37] D. Smith, A.G. Dean, N.G. Adams, J. Phys. D 7 (1974) 1944–1962.
[38] R. Plasil, J. Glosik, V. Poterya, P. Kudrna, M. Vicher, A. Pysanenko, in: S.L. Guberman (Ed.), Dissociative Recombination of Molecular Ions with Electrons, Kluwer, New York, 2003, pp. 249–263.
[39] C.D. Molek, J.L. McLain, V. Poterya, N.G. Adams, J. Phys. Chem. A 111 (2007) 6760–6765.
[40] N.G. Adams, L.M. Babcock, C.D. Molek, in: P. Armentrout (Ed.), Encyclopedia of Mass Spectrometry: Theory and Ion Chemistry, vol. 1, Elsevier, Amsterdam, 2003, pp. 555–561.
[41] A. Kallberg, in: A. Kallberg, E. Oppenheimer (Eds.), Manne Siegbahn Laboratory Annual Report 1999, Manne Siegbahn Laboratory, 2000, pp. 1–115.
[42] E. Herbst, J. Phys. Conf. Ser. 4 (2005) 17–25.
[43] W.D. Geppert, R.D. Thomas, A. Ehlerding, F. Hellberg, F. Osterdahl, M. Hamberg, J. Semaniak, V. Zhaunerchyk,M. Kaminska, A. Kallberg, A. Paal, M. Larsson, J. Phys. Conf. Ser. 4, London, 2005, pp. 26–31.
[44] B. Wang, C. Fockenberg, J. Phys. Chem. A 105 (2001) 8449–8455.
[45] K.H. Becker, R. Kurtenback, P. Wiesen, J. Phys. Chem. 95 (1991) 2390–2394.
[46] S.M. Anderson, A. Freeman, C.E. Kolb, J. Phys. Chem. 91 (1987) 6272–6277.
[47] R. Jenkins, R.W. Gould, D. Gedcke, Quantitative X-ray Spectrometry, vol. 20, Marcel Dekker, Inc., 1995.
[48] R.E. Rosati, R. Johnsen, M.F. Golde, J. Chem. Phys. 120 (2004) 8025–8030.
[49] J.W. McGowan, R.H. Kummler, F.R. Gilmore, Adv. Chem. Phys. 28 (1975) 379–422.
[51] J.M. Butler, L.M. Babcock, N.G. Adams, Mol. Phys. 91 (1997) 81–90.
[52] M.E. Jacox, J. Phys. Chem. Ref. Data Monograph 3, 1994.
[53] G. Herzberg, Molecular Spectra and Molecular Structure. III. Electronic Spectra and Electronic Structure of Polyatomic Molecules, D. Van Nostrand, Princeton, New Jersey, 1967.
[54] S.G. Westre, T.E. Gansberg, P.B. Kelly, L.D. Ziegler, J. Phys. Chem. 96 (1992) 3610–3615.
[55] D.R. Bates, Adv. Atom. Mol. Opt. Phys. 34 (1994) 427–486.
[56] J.E. Mann, J.D. Savee, R.E. Continette, J. Phys. Conf. Ser. (2008).
[57] C.H. Sheehan, J.-P. St.-Maurice, Adv. Space Res. 33 (2004) 216–220.
[58] L. Lehfaoui, C. Rebrion-Rowe, S. Laube, B.A. Mitchell, B.R. Rowe, J. Chem. Phys. 106 (1997) 5406–5412.
[59] T. Gougousi, M.F. Golde, R. Johnsen, Chem. Phys. Lett. 265 (1997) 399–403.
[60] N.G. Adams, D. Smith, E. Alge, J. Chem. Phys. 81 (1984) 1778–1784.
[61] D. Smith, P. Spanel, Int. J. Mass Spectrom. Ion Proc. 129 (1993) 163–182.
[62] M. Larsson, in: P.B. Armentrout (Ed.), The Encyclopedia of Mass Spectrometry: Theory and Ion Chemistry, Elsevier, 2003, pp. 195–199.
[63] R. Johnsen, J. Phys. Conf. Ser. (2005) 83–91.
[64] H.A. Wooten, http://www.cv.nrao.edu/~awootten/allmols.html, 2002.
[65] D.R. Bates, H.S.W. Massey, Phil. Trans. Roy. Soc. A239 (1943) 269–304.
[66] R.E. Olson, J. Chem. Phys. 56 (1972) 2979–2984.
[67] J.T. Moseley, R.E. Olson, J.R. Peterson, Case Stud. Atomic Phys. 5 (1975) 1–45.
[68] B.R. Rowe, F. Vallee, J.L. Queffelec, J.C. Gomet, M. Morlais, J. Chem. Phys. 88 (1988) 845–850.
[69] L. Vejby-Christensen, L.H. Andersen, O. Heber, D. Kella, H.B. Pedersen, H.T. Schmidt, D. Zajfman, Ap. J. 483 (1997) 531–540.
[70] M.J. Jensen, R.C. Bilodeau, O. Heber, H.B. Pedersen, C.P. Safvan, X. Urbain, D. Zaijman, L.H. Andersen, Phys. Rev. A 60 (1999) 2970–2976.
[71] S. Rosen, A.M. Derkatch, J. Semaniak, A. Neau, A. Al-Khalili, A. Le Padellec, W.S.L. Vikor, R. Thomas, H. Danared, M.af. Ugglas, M. Larsson, Faraday Discuss. 115 (2000) 295–302.
[72] L.H. Andersen, O. Heber, D. Kella, H.B. Pedersen, L. Vejby-Christensen, D. Zajfman, Phys. Rev. Lett. 77 (1996) 4891–4894.
[73] A. Neau, A.A. Khalili, S. Rosen, A. Le Padellec, A.M. Derkatch, W.S.L. Vikor, J. Semaniak, R. Thomas, M.B. Nagard, K. Anderson, H. Danared, M.af. Ugglas, J. Chem. Phys. 113 (2000) 1762–1770.
[74] M.J. Jensen, R.C. Bilodeau, C.P. Safvan, K. Seiersen, L.H. Andersen, H.B. Pedersen, O. Heber, Ap. J. 543 (2000) 764–774.
[75] V. Tarnovsky, H. Deutsch, K. Becker, Int. J. Mass Spectrom. 167 (1997) 69–78.
[76] O. Asvany, I. Savic, S. Schlemmer, D. Gerlich, Chem. Phys. 298 (2004) 97–105.